CASE 48

Optimization of a Clutch Disk Torsional Damping System Design

Abstract: During the development of a new clutch disk damping system and after three months of hard work, the engineering team got stuck with unsatisfactory system performance (rattle noise) despite the help of a computer simulation software. The only alternative seemed to be using a more expensive damping concept, but that option would increase part cost by $200 plus development cost. The team then decided to try Taguchi's robust engineering optimization approach. In just two weeks we got a gain of 4.6 dB for the SN ratio. That allowed us to keep the system proposed initially, thus avoiding the cost increase and keeping the development schedule on track. Perhaps even more important, we can now apply our engineering knowledge more effectively and make better use of the computer simulator, which results in a faster and more reliable development process.

1. Introduction

More and more attention is being paid to audible noise caused by torsional vibrations in the engine–clutch–transmission–rear axle system (the drive train). On the one hand, modern automotive design is producing stronger mechanical excitation due to more powerful engines; on the other hand, transmissions that have been optimized for weight and efficiency are highly sensitive to excitation. This situation brings a number of comfort problems, including rattle noise.

Many sources of excitation must be considered related to torsional vibrations. The main source is engine irregularity resulting from the ignition cycle. This basic excitation in the motor vehicle drive train is the focus of this study. Irregular ignition or even misfiring can also lead to serious vibration problems, but those factors were not included in this work because they can usually be eliminated by optimizing the ignition itself. The main source of excitation for torsional vibrations is the fact that engine ignition is not a continuous process but rather is discrete. That is also the primary cause of low-speed gear rattle. The basic principles involved in this phenomenon are described below.

Torque at the crankshaft is a periodic function of time. The torque curve is determined by the gas forces in the cylinder, by the geometry of the crank drive, and by the acceleration moments of the crank drive as it changes mass moments of inertia during one rotation. Significant mass forces occur at higher speeds only, where they can even become dominant. Because gear rattle occurs primarily at low engine speeds, inertial forces are negligible for our observations. That yields the very simple torque relationship shown in Figure 1.

According to that equation, the time-dependent torque acting on the crankshaft is the product of piston displacement, a geometric factor dependent on the angle of the crankshaft and the pressure curve of the cylinder. The graph shown at the bottom of Figure 1 illustrates that principle for one cylinder. In a six-cylinder engine, that curve is repeated three times per revolution.

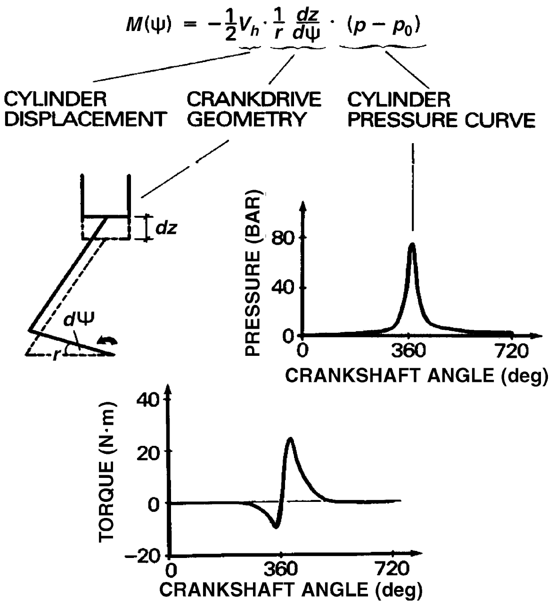

Figure 1
Engine excitation due to gas forces

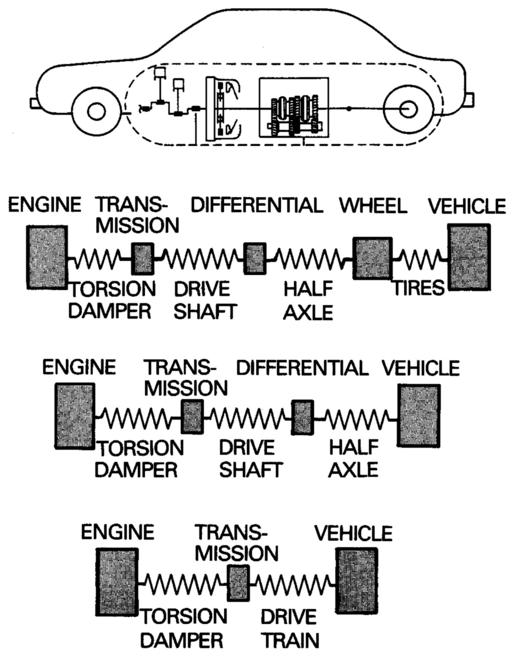

Figure 2
Analytical model for vehicle drive train vibrations

Peak torque magnitude (M) by itself does not reveal anything about engine irregularity. This value is based on the mass moment of inertia, J_m, of the crankshaft, together with components such as the flywheel and the clutch, which are attached to it rigidly. The angular acceleration, $\Omega_{\cdot m}$, is determined using the equation

$$M = J_m \Omega_{\cdot m}$$

That factor exhibits an almost constant amplitude at the low speeds in which we are interested. The curve for the angular velocity or the speed as a function of time can be plotted using integration:

$$\Omega_m = \int \Omega_{\cdot m}\, dt$$

A vehicle drive train represents a torsional vibration system. It can be described roughly as a chain of rotating inertia and torsion springs. We can assume that we are dealing with a linear chain (Figure 2). For purposes of clarity, we will try to get by with as few different rotating inertia and torsion springs as possible. This type of simple model provides adequate information for many vibration problems. Of course, it is important to emphasize that it cannot be used to study all drive train problems.

Figure 3 shows the possible vibration modes for a simple three-mass vibration system. In the case of rattle noise, the transmission vibrates at high amplitudes. Natural frequencies of 40 to 80 Hz are typical. This vibration mode occurs in the case of gear rattle noise.

Whenever engine irregularity excites the drive train vibration system, resonance can occur if the excitation frequency equals the natural frequency. Because engine excitation is not sinusoidal, additional high-frequency components must occur in the excitation, but their intensity generally decreases with increased frequency. Rattle vibration is excited primarily by the third and sixth orders in a six-stroke engine. Associated resonance speeds typically occur in the approximate range 700 to 2000 rpm. The lower the gear selected, the higher those speeds.

In theory, there are several options for modifying the vibration performance of a vehicle drive train in order to reduce undesirable torsional vibrations.

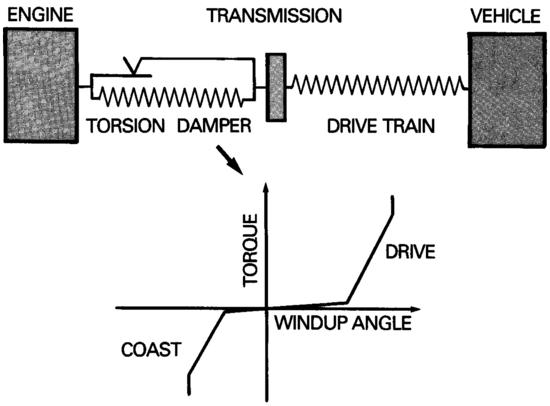

Figure 3
Torsion damper characteristic curve in analytical model

Unfortunately, however, compelling engineering considerations prevent us from changing most of the components making up the drive train. Therefore, with the exception of the flywheel mass, it is hardly possible to change the mass moments of inertia involved in the system, nor is it readily feasible to alter the spring rates (stiffness) of the tires, half axles, and drive shafts. Consequently, the only actual option left to target for positive change is the connection between the engine and the transmission.

An appropriate damped, torsionally elastic coupling (torsional damper) can be used to shift the resonance speeds and damp resonance amplitudes. Generally, gear rattle in the drive, coast, and idle modes requires different torsional elasticity and damping characteristics. Consequently, most torsion dampers include precisely tuned multistage characteristic curves, with each stage optimized individually for its respective load ranges.

Based on a calculated example, vibration performance can be influenced by changing torsional spring rate and damping. Each section of the matrix graph shows the vibration amplitude of the engine and the transmission speed plotted as a function of the mean engine speed. Engine speed is plotted as a solid line, and transmission speed is plotted as a dashed line. Each section was based on the calculation for a torsional damper with different frictional hysteresis and torsional spring rate.

We note that vibration isolation does not occur until we reach the speed range above natural frequency in the 2000 rpm range. If we reduce the torsional spring rate, we can shift the resonance to lower speeds and introduce the vibration isolation range sooner. At very low torsional spring rates of about 1 N · m/deg, the vibration amplitude also decreases significantly in the resonance range. With that design, the very flexible coupling passes hardly any vibrations at all through to the rest of the drive train. This would constitute the ideal torsion damper.

Unfortunately, it is impossible to accommodate this type of flat spring rate in the space available for installing the clutch. It is impossible to achieve vibration insulation in drive mode over the engine speed range using an elastic coupling such as a conventional torsion damper. As a result, torsion damper tuning always represents a compromise. Low hysteresis results in high resonance amplitudes at low speeds and good vibration insulation at high speeds, whereas high hysteresis leads to rigid performance. If a satisfactory compromise proves impossible, other vibration damping procedures must be adopted.

By using traditional, knowledge-guided one-factor-at-a-time experiments using computer simulation, we have tried successive design–prototype–test cycles. But after three months we still did not find an acceptable solution for the aforementioned compromise, and the design release deadline was too close to venture major changes. Then one of the team members suggested the application of robust engineering in the simulation analysis, whose results we now report.

2. Experimental Procedure

Scope of Experiment

Figure 4 shows the engineering system under study. Its parts are spring set and friction components. System frontiers are, at the input, the engine flywheel, and at the output, the input transmission shaft.

System Function

The objective function is to minimize the angular variation from the engine while transferring torque through the system. The basic function (work) is to

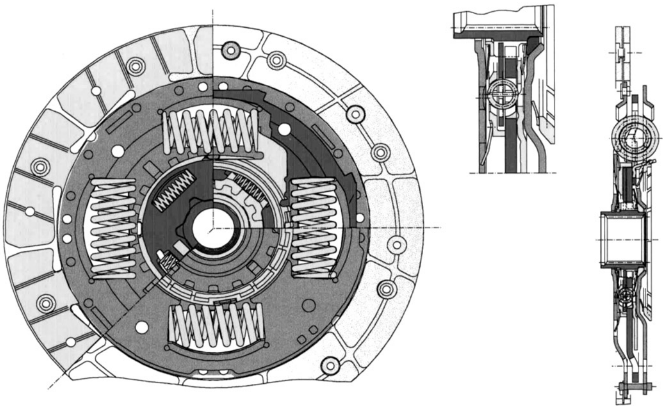

Figure 4
Damping system

attenuate angular variation. A P-diagram and ideal function are shown in Figure 5.

Since the function of the damping system is to attenuate the angular variation generated by the engine, we defined as the signal factor, M, the angular variation in the flywheel, and as the response, y, the attenuated angular variation, which ideally should be equal to M. Graphically, the ideal function is a straight line through zero, with unity angular coefficient (Figure 6).

The following relationship holds for the system:

$$y = \Delta - M$$

where y is the attenuated angular variation, Δ the angular variation at the output, and M the angular variation at the input. If we want the ideal behavior $y = M$, Δ must be zero. Therefore, because of this one-to-one relationship between y (dynamic characteristic) and Δ (smaller-the-better characteristic), for the sake of easier analysis, we decided to work on the minimization of Δ. We found that approach acceptable in this case, because one can see that Δ is the single and only functional symptom of y and is measured in the same unit scale.

Our response y becomes Δ, the angular variation at the output of the damping system (which, by the

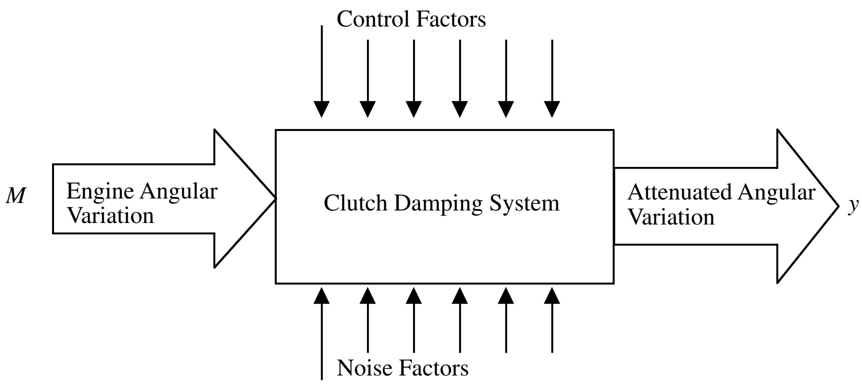

Figure 5
P-diagram for the engineering system

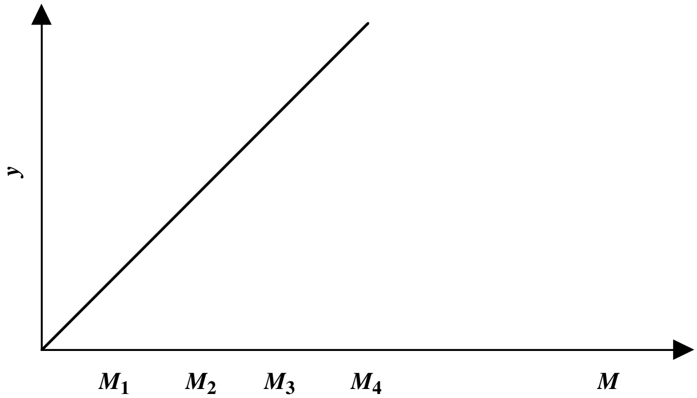

Figure 6
Ideal function

way, is the software response) and is analyzed as a smaller-the-better characteristic because it represents the angular variation that was not attenuated by the system and was released at the output (whose ideal value is zero).

Signal and Noise Factor Strategies

The signal, M, is a function of the engine speed; therefore, the software was fed with a curve of angular variation from 500 to 2500 rpm. To analyze the software output, we took the response y (Δ) in incremental steps of 50 rpm, starting at 750 rpm (engine idle speed). For each run of the orthogonal array, a smaller-the-better SN ratio was calculated from the 10 highest peak values of the response curve, in selected points of interest in the rpm range. (See the example in Figure 7 and Table 1.)

Besides sweeping the input signal, M (which for smaller-the-better calculations can also be regarded as noise), we simulated additional noise factors related to deterioration and variability existing in the manufacturing environment (Table 2).

Control Factors

The control factors are as follows:

- *Elastic constant* (K) *of the spring* (A). Six levels are included in order to explore the design space as much as possible.
- *Angle at the beginning of the second friction level* (B). In the damping system under study, it is possible to use two friction levels along the total work angle. The control factor, B, is of great importance to identify the range of work angle for each friction level, or even to answer the following question: Do we need two friction levels? Therefore, we considered the maximum work angle of 20° divided into three levels.
- *Second friction.* As described above, the system under study allows the use of two friction levels along its range of 20°. To identify the value to be adopted, three wide (although feasible) levels were defined, from low to high.
- *First friction.* The basic requirement for the friction system to work is that the first level must be smaller than the second one, so the three levels for factor D were defined as a percentage of factor C.

These control factors were assigned to an orthogonal L_{18} array (Table 3).

3. Experimental Data and Analysis Using a Smaller-the-Better SN Ratio

For each combination of L_{18}, we obtained a group of data composed by the highest 10 peaks, under each noise condition N_1 and N_2 (Table 4). See Tables 5 to 7 for data analysis.

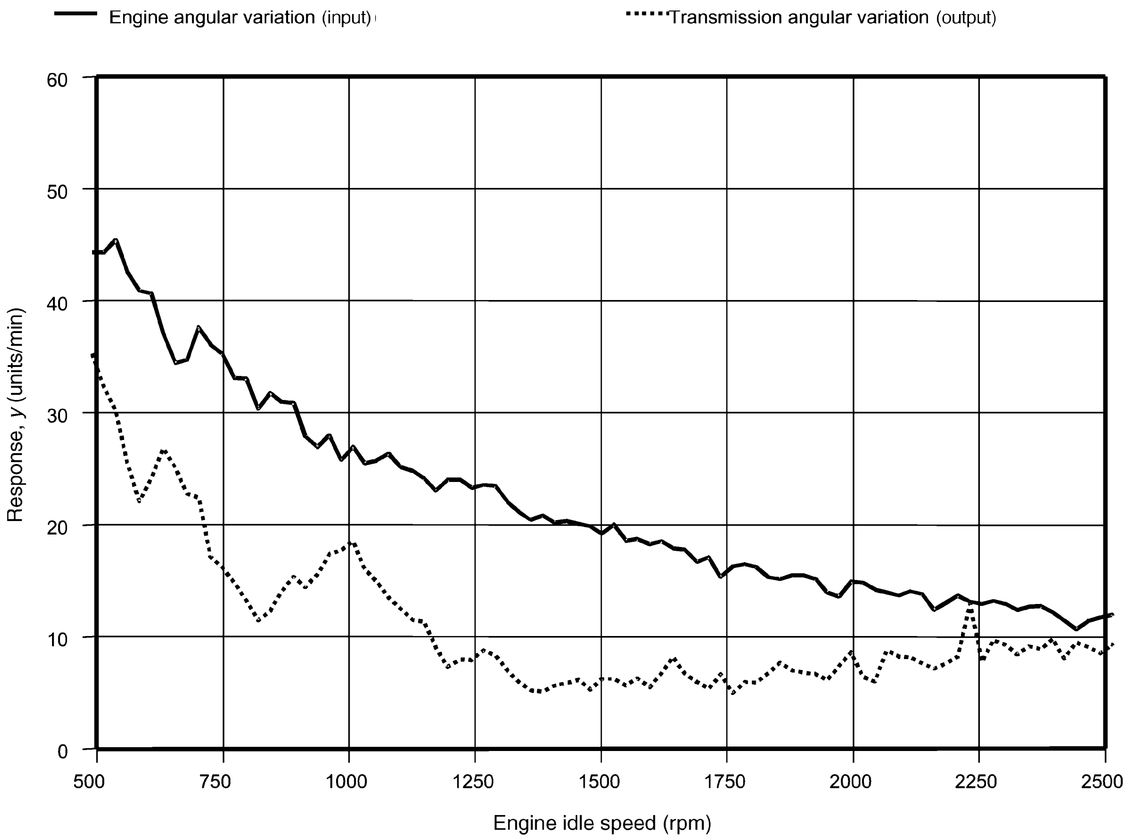

Figure 7
Example of simulator response

Table 1
Example of response for each experimental run

Run	Signal (rpm)	Response, y (units/min)
25	M_7: 1050	16.5
27	M_6: 1000	18
28	M_5: 950	17.5
31	M_4: 900	16
⋮		

4. Results

The SN results (in decibels) are:

Initial configuration:	−23.46
Optimum configuration ($A_6B_3C_1D_1$):	−18.58
Confirmed by simulation:	−18.90
Gain:	4.56

As expected, due to the good correlation between the simulator and reality, the SN gain was confirmed subsequently in vehicle testing. Figures 8 and 9 show the positive impact obtained in the damping system performance by comparing the initial situation (Figure 8) with the optimized design (Figure 9).

Table 2
Compound noise

Compound Noise[a]	Noise Factor N_1 (y high)	Noise Factor N_2 (y low)
Variation of K_{spring}	Control fator *A* value, minus *X*% fatigue	Control factor *A* vaue, plus *X*% manufacturing variation
Variation of $K_{vehicle}$	Min.	Max.

[a] *K*, elastic constant.

With that optimization, the subjective evaluation rating improved from 4.0 (rated as failure by all customers) to 5.5 (rated as disturbing by some customers). That improvement was enough to keep us from having to adopt a more complex and expensive damping system that would add $200 to the system cost. To achieve the development target grade of 7.0 (satisfactory to noticeable by all customers, but not causing disturbance), we decided to increase the mass of the engine flywheel by 20%, with minimum impact on piece cost. Those actions combined were effective, and the development schedule was kept on track.

5. Conclusions

In the process of conventional design using simulation, the control factors were being analyzed separately, one at a time. Although the computer analysis was fast, the responses that we obtained were far from optimum. Thus, after vehicle prototype testing, we had to get back to a new cycle of simulation, prototype construction, and evaluation in the vehicle, which increased the time and cost of development.

With the use of the robust engineering methodology, the technology under study (clutch damping system) could be optimized quickly using the simulator and there was no need to build more than one physical prototype. In that way, besides system performance quality improvement, we were able to achieve a faster and less expensive development cycle.

This robust engineering study also allowed us to maintain the low-complexity system, thus avoiding an apparently unavoidable cost increase that would occur by using a more sophisticated damper. We

Table 3
Control factors and levels

Level	Control Factor *A*: Spring's *K*	*B*: Angle to Second (deg) Friction Starts	*C*: Second Friction (N)	*D*: First Friction (% of *C*)
1	4.6	0	3	25
2	9.2	7	15	50
3	13.8	14	27	75
4	18.4			
5	23			
6	27.6			

Table 4
L_{18} orthogonal array and responses under noise extremes

	Factor				y at:	
No.	*A*	*B*	*C*	*D*	N_1	N_2
1	4.6	0°	3	0.75	120 95 60 37 36 26 22.5 22.5 21 21	105 65 60 39 28 26.5 21 18.5 18 16.5
2	4.6	7°	15	7.5	49 44 34 29 26 26 26 23 23 23	41.5 41 30.5 27 26 24.5 24 24 22 21
3	4.6	14°	27	20.25	30 29.5 29 29 27 26 23.5 23.5 23 21.5	29.5 29 25.5 25 24.5 22.5 22.5 21 21 20.5
4	9.2	0°	3	1.5	97 76 62 38 34 26.5 22.5 21 18.5 14.5	87 66 54 39 28 27 21 18 13 11
5	9.2	7°	15	11.25	49 44.5 33 30 26 26 25 23.5 23 21.5	42 41 31 26 26 24 24 23.5 22.5 20.5
6	9.2	14°	27	6.75	30.5 29.5 29 27.5 26 25.5 23.5 23 22 21.5	28.5 25.5 25.5 24.5 22.5 22.5 21 21 20.5 20
7	13.8	0°	15	3.75	49.5 44 33 29 26.5 26 23 23 21.5 21.5	23.5 23 22 19.5 19 18 15 15 14 14
8	13.8	7°	27	13.5	30 29.5 29 27 25.5 25 23 23 22 19.5	26 24.5 23.5 22.5 21 20 19 18 17.5 17
9	13.8	14°	3	2.25	60 54 50.5 37 36 21 15 11.5 10.5 10	13.5 11 11 10.5 8.5 7.5 5.5 5.5 5 5
10	18.4	0°	27	20.25	30.5 27 25 23.5 21.5 20 19 18.5 17 16.5	28.5 26 24.5 22.5 20.5 20 19.5 19 16.5 16
11	18.4	7°	3	0.75	12 10 9.5 6.5 6 4.5 4.5 4 3.5 3.5	12.5 11.5 10 7 6.5 5 5 4 4 3.5
12	18.4	14°	15	7.5	21 20 20 18 15 13.5 13.5 13.5 13.5 13.5	28 25.5 22.5 20.5 19.5 18 16.5 16 15.5 15
13	23	0°	15	11.25	26.5 23 23 20.5 18.5 18 15.5 14 14 13.5	24 23 22 20 19.5 18 16 15 14.5 14.5
14	23	7°	27	6.75	30 27 24 23.5 21 19.5 18.5 17 17 16.5	28.5 25.5 22.5 20.5 19.5 19 18 16.5 16 16
15	23	14°	3	1.5	12 10 9 6 5.5 4 4 4 3.5 3.5	13.5 11.5 9.5 6.5 6.5 4.5 4 3.5 3.5 2.5
16	27.6	0°	27	13.5	30 27 25 23 21 20 19 18.5 18 17	28.5 26 24.5 22 20.5 20.5 19.5 18.5 17 16
17	27.6	7°	3	2.25	14.5 13 12 8.5 8 6 5.5 4.5 4 4	15.5 15 13 9 8 6.5 5.5 5.5 4.5 4
18	27.6	14°	15	3.75	15 13.5 13 9 8 6.5 5.5 5 4.5 4	15.5 14.5 13.5 9.5 9.5 7 6.5 5.5 5 4.5

Table 5
Control factors and calculated values of SN and average (smaller-the-better)

No.	Factor *A* 1	*B* 3	*C* 4	*D* 5	SN (dB)	Average
1	1	1	1	1	−34.66	42.93
2	1	2	2	2	−29.85	29.23
3	1	3	3	3	−28.30	25.15
4	2	1	1	2	−33.52	38.70
5	2	2	2	3	−29.83	29.10
6	2	3	3	1	−28.07	24.48
7	3	1	2	1	−28.40	24.00
8	3	2	3	2	−27.62	23.13
9	3	3	1	3	−28.52	19.43
10	4	1	3	3	−27.06	21.58
11	4	2	1	1	−17.50	6.65
12	4	3	2	2	−25.51	17.93
13	5	1	2	3	−25.82	18.65
14	5	2	3	1	−26.76	20.80
15	5	3	1	2	−17.30	6.35
16	6	1	3	2	−27.04	21.58
17	6	2	1	3	−19.51	8.33
18	6	3	2	1	−19.85	8.75
Grand averages:					−26.40	21.48

Table 6
Response table for the SN ratio

No.	Factor *A*	*B*	*C*	*D*
1	−30.94	−29.42	−25.17	−25.87
2	−30.47	−25.18	−26.54	−26.81
3	−28.18	−24.59	−27.48	−26.51
4	−23.35			
5	−23.29			
6	−22.13			
Diff.	8.80	4.82	2.31	0.94

Table 7
Response table for the mean

No.	Factor *A*	*B*	*C*	*D*
1	32.43	27.90	20.40	21.27
2	30.76	19.54	21.28	22.82
3	22.18	17.01	22.78	20.37
4	15.38			
5	15.27			
6	12.88			
Diff.	19.55	10.89	2.39	2.45

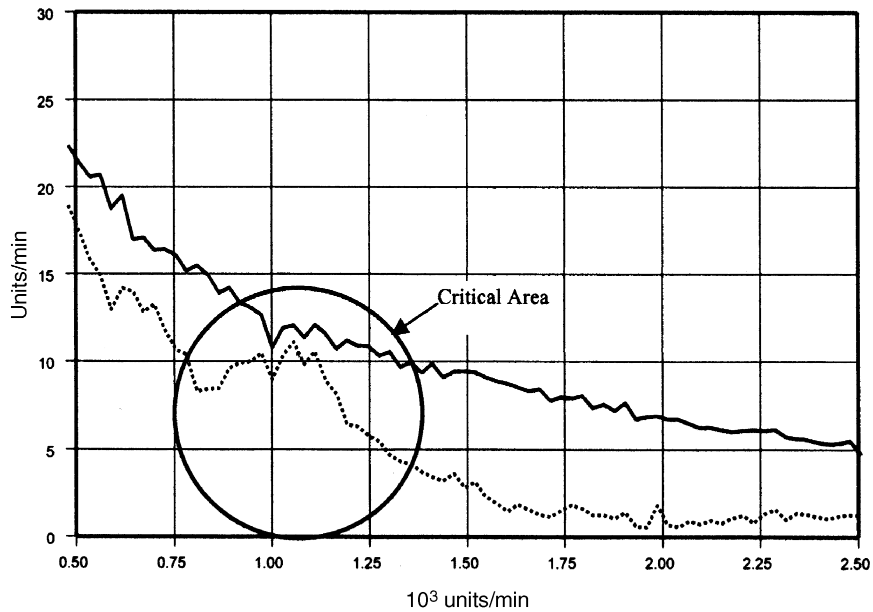

Figure 8
Damping system performance before study

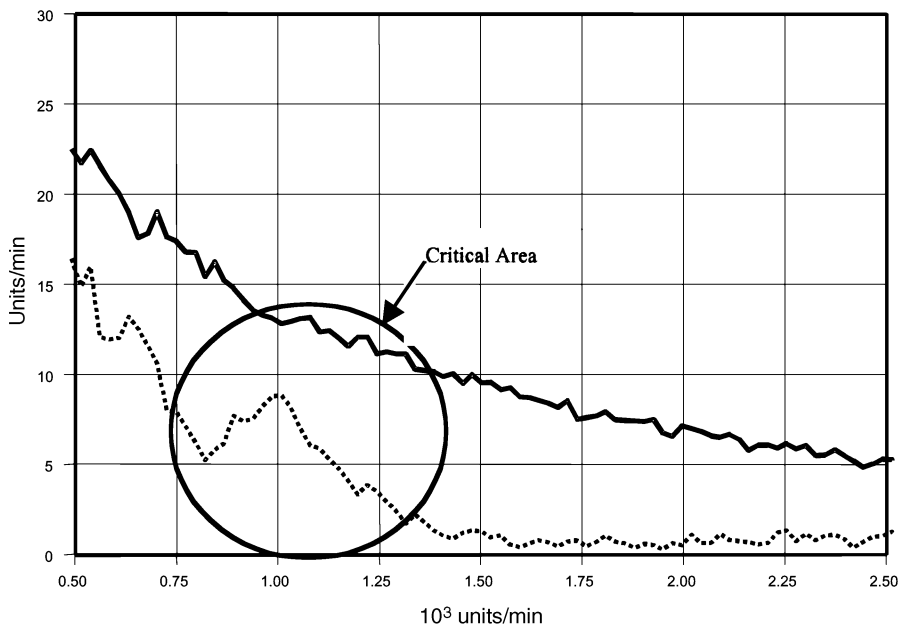

Figure 9
Damping system performance after study

also got rid of a critical development schedule pressure, because a solution that at first seemed impossible could quickly be identified.

Perhaps even more important, from now on we can more effectively apply our engineering knowledge and make better use of the computer simulator, which should result in faster and more reliable development cycles in the future.

This case study is contributed by Luiz H. Riedel, Claudio Castro, Nélio de Lucia, and Eduardo Moura.